Power corrections in collider processes

Paolo Nason,

INFN, sez. di Milano Bicocca

in collaboration with: Fabrizio Caola, Silvia Ferrario Ravasio,
Giovanni Limatola, Kirill Melnikov, Melih Arslan Ozcelik, Giulia Zanderighi

Universität Wien, 4/10/2024

UNIVERSITA' DEGLI STUDI DI MILANO BICOCCA

INFN Istituto Nazionale di Fisica Nucleare

ACCADEMIA NAZIONALE DEI LINCEI

Alexander von Humboldt Stiftung/Foundation

Outline

- Power corrections in collider processes
- Renormalons and linear power corrections
- Massless partons
- Massive partons
- e^+e^- annihilation: shape-variables in the 3-jet region.
- Fits to e^+e^- data.

Power corrections for collider processes

- Little is known about power corrections in QCD processes.
- Some simpler processes admit an OPE (the total cross section in e^+e^- annihilation and similar processes, DIS-like processes, B meson decays ...) so that power corrections can be parametrized.
- For the complex collider processes one worries about the presence of linear power corrections, i.e. corrections of the order of Λ/Q, since these could be at the percent level, that is the accuracy one is aiming for at the HL LHC.
- One instrument for the investigation of linear power correction is the study of renormalons in the large b_0 approximation.

ABC of I.R. Renormalons

All-orders contributions to QCD amplitudes of the form

$$\int_0^m \mathrm{d}k^p\, \alpha_s(k^2) = \int_0^m \mathrm{d}k^p\, \frac{1}{b_0 \log(k^2/\Lambda^2)}$$
$$= \int_0^m \mathrm{d}k^p \frac{\alpha_s(m^2)}{1 + b_0\alpha_s(m^2)\log\frac{k^2}{m^2}}$$
$$= \alpha_s(m^2) \sum_{n=0}^{\infty} (2b_0\alpha_s(m^2))^n \int_0^m \underbrace{\mathrm{d}k^p \log^n \frac{m}{k}}_{p^n n!} .$$

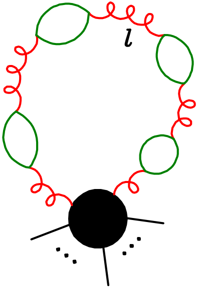

Asymptotic expansion.

- Minimal term at $n_{\min} \approx \frac{1}{2pb_0\alpha_S(m^2)}$.
- Size of minimal term: $m^p\alpha_s(m^2)\sqrt{2\pi n_{\min}}e^{-n_{\min}} \approx \Lambda^p$.

Large-n_f all-order result

Given an (IR safe) observable O, we introduce the notation

- Φ_B, phase space;
- Φ_g, phase space for the emission of one massive gluon with mass λ,
- $\Phi_{q\bar{q}}$, phase space for the emission of a $q\bar{q}$ pair

the all-order result can be expressed in terms of

- $\sigma_B(\Phi_B)$, the differential cross section for the Born process;
- $\sigma_v(\lambda, \Phi_B)$, the virtual correction to the Born process due to the exchange of a gluon of mass λ;
- The real cross section $\sigma_{g^*}(\lambda, \Phi_{g^*})$, obtained by adding one massive gluon to the Born final state;
- The real cross section $\sigma_{q\bar{q}}(\Phi_{q\bar{q}})$, obtained by adding a $q\bar{q}$ pair, produced by a massless gluon, to the Born final state;

Large-n_f all-order result

Defining:

$$
\begin{aligned}
T_O(\lambda) &= \overbrace{V_O(\lambda) + R_O(\lambda)}^{\text{result for a gluon with mass } \lambda} + \overbrace{\Delta_O(\lambda)}^{\text{Seymour,PN1995}}, \\
V_O(\lambda) &= \int \mathrm{d}\Phi_{\mathrm{b}}\, \sigma_{\mathrm{v}}^{(1)}(\lambda^2, \Phi_{\mathrm{b}})\, O(\Phi_{\mathrm{b}}), \\
R_O(\lambda) &= \int \mathrm{d}\Phi_{g^*}\, \sigma_{g^*}^{(1)}(\lambda^2, \Phi_{g^*}) O(\Phi_{g^*}), \\
\Delta_O(\lambda) &= \frac{3\pi\lambda^2}{\alpha_S T_F} \int \mathrm{d}\Phi_{q\bar{q}} R_{q\bar{q}}(\Phi_{q\bar{q}}) \delta(m_{q\bar{q}}^2 - \lambda^2) \left[O(\Phi_{q\bar{q}}) - O(\Phi_{g^*})\right]
\end{aligned}
$$

The Δ term vanishes if the observable is totally inclusive in the radiated partons.

It turns out that a linear term in λ in the expansion of $T(\lambda)$ around zero is associated with linear renormalons.

Large-n_f all-order result

The all-order result is given by

$$\langle O \rangle = B_O - \int \mathrm{d}\lambda \frac{\mathrm{d}T_O(\lambda)}{\mathrm{d}\lambda} \underbrace{\frac{1}{\alpha_S} \overbrace{\left[\frac{1}{\pi b_0} \arctan \frac{\pi b_0 \alpha_S}{1 + b_0 \alpha_S \log \lambda^2/\mu_C^2}\right]}^{\text{Beneke,98}}}_{\alpha_{\mathrm{s,eff}}(\lambda)/\alpha_s}$$

It is easy to show that a linear λ term in $T_O(\lambda)$ leads to a factorial growth related to a linear IR renormalon. In fact

$$\int \mathrm{d}\lambda \left[\frac{1}{\pi} \arctan \frac{\pi b_0 \alpha_S}{1 + b_0 \alpha_S \log \lambda^2/\mu_C^2}\right] = \frac{1}{\pi} P \int_0^\infty \mathrm{d}t \frac{\exp\left(-\frac{t}{2 b_0 \alpha_S}\right)}{1-t} - \exp\left(-\frac{1}{2 b_0 \alpha_s}\right) + \text{terms analytic in } \alpha_S. \tag{1}$$

Large-n_f all-order result

- We have a well-defined procedure for the computation of the T function..
- Can be computed semi-numerically. This approach has been followed in
  - Ferrario Ravasio, Oleari, PN,2019 for studies related to the top mass measurements.
  - Ferrario Ravasio, Limatola, PN,2021 for showing the absence of linear corrections to the p_T spectrum of the Z in hadronic collisions.

Gavin Salam had often shown an argument in favour of the presence of linear power corrections to the inclusive p_T spectrum of the Z boson, based upon the fact that the soft radiation associated to this process is not azimuthally symmetric. Our attemt to actually compute such an effect in a model theory gave negative results.

It is however difficult, numerically, to show the absence of a correction, especially in this case where the cancellation of soft-collinear divergence between the virtual (computed analytically) and real (computed numerically) is involved.
Analytic results were found:

- Analytic approach for massless partons:
  Caola,Ferrario Ravasio,Limatola,Melnikov, PN 2021,[2108.08897], same authors + Ozcelik 2022[2204.02247]
- Analytic approach for massive partons:
  Makarov, Melnikov, Ozcelik, PN, 2023, [2302.02729], 2023[2308.05526], 2024[2408.00632]

Cancellation of linear NP terms

Our findings can be summarized as follows:

- Consider a process, described by a cross section (with no radiation) $B(p_1, \ldots p_n)$ where p denotes a set of fixed external momenta, with $p_3 \ldots p_n$ colourless particles, and p_1, p_2 massless quark antiquark (final-final or initial-initial) or quark-quark (initial-final) pair.
- Assume that we emit a massive gluon of mass λ and momentum k, and we have a smooth (in a sense to be clarified afterwards), IR safe mapping from the full real emission configuration to the underlying Born one.

Then:

- No linear λ sensitivity arises from virtual corrections
- No linear λ sensitivity arises from the real contributions due to an unrestricted integration in k at fixed underlying Born kinematics.

The result is based upon two observations:

- Virtual corrections have no linear power corrections.
  One can show that the virtual integrals give rise to constants, logs and double logs of λ, but no linear terms in λ.
- Writing the real emission term in a factorised form:

$$\mathrm{d}\Phi_g = J \times \mathrm{d}\Phi_B \frac{\mathrm{d}^3 k}{k_0} \tag{2}$$

  through the choice of a mapping to an underlying Born $\Phi_g \leftrightarrow \{\Phi_B, k\}$, (or choice of a recoil scheme),
  it can be shown that if the mapping is linear in k for small k, no linear renormalons are present after the k integration. So: in inclusive cross sections at fixed undelying Born no renormalons are present.

Virtual corrections

- Virtual corrections due to the exchange of a massive gluon emitted by massless partons never lead to linear terms in the mass λ. Besides verifying this in the practical case, this can be proven by considering that the Passarino-Veltman reduction procedure never leads to linear terms in λ, and by examining the IR divergent scalar integrals.

Hard collinear region

- Hard, collinear divergences do not lead to linear terms λ. In fact, defining Sudakov variables for the gluon momentum

$$k = zp_1 + \beta p_2 + k_\perp, \qquad \beta = \frac{k_\perp^2 + \lambda^2}{z 2 p_1 \cdot p_2},$$

collinear integrals have the form

$$\int \mathrm{d}k_\perp^2 \frac{P(k_\perp)}{\left(k_\perp^2 + (1+z)\lambda^2\right)^i}, \qquad i = 1, 2.$$

$P(k_\perp)$, for small $k_\perp$, can start with a constant if $i = 1$, and must start with a term bilinear in $k_\perp$ or proportional to λ^2 if $i = 2$.
If the mapping near the collinear region is linear in $k_\perp$, no linear terms in λ can arise, since subleading terms in $k_\perp$ are odd, and vanish by azymuthal integration.

The soft region

The soft region leads to integrands of the form

$$\int \frac{\mathrm{d}^3\vec{k}}{\omega} P(k)\left[\frac{1}{(2p_1\cdot k+\lambda^2)(2p_2\cdot k+\lambda^2)},\quad \frac{\lambda^2}{(2p_{1/2}\cdot k+\lambda^2)^2}\right]$$

It is easy to see that (in the p_1, p_2 dipole CM)

$$p_1\cdot k = \frac{Q}{2}\omega(1-\beta cos\theta) \geq \frac{Q}{2}\omega(1-\beta) \geq \frac{Q\lambda^2}{4\omega} \geq \frac{Q\lambda}{4}\,,$$

so, the denominators scale at worse like λ, so does ω and $|\vec{k}|$. By power counting the second integral scales like λ^2, while the first one scales like 1.

In the first integral, subleading terms in ω, for example, may lead to terms linear in λ.

We now consider the k integral in the soft region at fixed underlying Born. We assume that the mapping from the underlying Born phase space to the full phase space is smooth for small k, in the sense that

$$p_i^\mu = \tilde{p}_i^\nu + T_i^{\mu\nu} k_\nu + \mathcal{O}(\omega^2)$$

where $\tilde{p}$ are the underlying Born momenta. The "dangerous" soft integral gives rise to terms of the form

$$\frac{1}{p_1 \cdot k + \lambda^2} = \frac{1}{\tilde{p}_1 \cdot k}\left[1 - \frac{k T_i k + \lambda^2}{\tilde{p}_1 \cdot k} + \ldots\right]$$

so that

$$\frac{1}{(p_1 \cdot k + \lambda^2)(p_1 \cdot k + \lambda^2)} = \frac{1}{\tilde{p}_1 \cdot k \, \tilde{p}_2 \cdot k}\left[1 - \sum_{i=1,2} \frac{k T_i k + \lambda^2}{\tilde{p}_i \cdot k} + \ldots\right]$$

where ... indicate terms subleading by power counting.

But, for collinear safety, $kTk \propto \tilde{p}_1 \cdot k \; \tilde{p}_2 \cdot k$, since it must vanish in both collinear limits. For example, $T_1 k$ must vanish if k is collinear to p_2, because in this case $p_1 = \tilde{p}_1$, and must be proportional to $\tilde{p}_1$ if k is collinear to p_1. Thus we end up having to worry about the following integrals

$$\int \frac{\mathrm{d}^3\vec{k}}{\omega} \left[\frac{1}{\tilde{p}_1 \cdot k \, \tilde{p}_2 \cdot k}, \quad \frac{k \cdot v}{\tilde{p}_1 \cdot k \, \tilde{p}_2 \cdot k}, \quad \frac{\lambda^2}{(\tilde{p}_1 \cdot k)^2 \, \tilde{p}_2 \cdot k} \right],$$

where v is a generic vector. Notice that one should also worry about the Jacobian, when changing integration variables from p, k to $\tilde{p}, k$. However, if the mapping is smooth in k, such change contributes at most a linear term, i.e. can be lumped into the $k \cdot v$ term.

By direct calculation, it can be easily seen that the above integrals do not yield linear terms in λ.

Consequences

Old and new results can be derived:
Linear corrections are absent in

- DIS (must be the case because of the OPE)
- Drell-Yan total cross section [Beneke and Braun]
- Drell-Yan rapidity distribution [Dasgupta]
- Dreal-Yan double differential cross section in transverse momentum and rapidity distribution of the pair (new)
- In e^+e^-, shape variables power corrections can be computed also in the 3-jet regime!
  Before they had been computed only in the 2-jet limits, with the only exception of the C-parameter in the 3-jet symmetric limit [Luisoni,Monni,Salam,2019]

The results on DIS and Drell-Yan follow because on can find an appropriate mapping that also maintains fixed Q^2 and x_{bj} for DIS, and the Drell-Yan pair kinematics for Drell-Yan.

consequences: Shape Variables

We investigating the structure of linear renormalons in the three jet region by computing the cross section for the process $\gamma^* \to q\bar{q}\gamma$

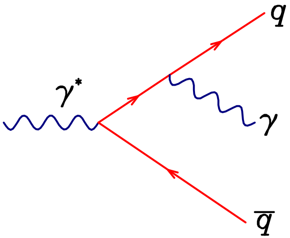

including gluonic corrections in the large n_f limit.

Our new analytic findings can also be applied to shape variables.

The large-n_f, $T_O(\lambda)$ result can also be written as

$$T_O(\lambda) = N\int \mathrm{d}\Phi_3 \left\{ \int \mathrm{d}\Phi_k^{(\lambda)} M_{\mu\nu}(k)\left[\int \mathrm{d}\Phi_{\text{split}} \overbrace{P^{\mu\nu}_{\text{split}}(O_5 - O_4)}^{\Delta(\lambda)} + \overbrace{O_4 g^{\mu\nu}}^{R(\lambda)} \right] + \overbrace{V_\lambda O_3}^{V(\lambda)} \right\}.$$

where $O_{3..5}$ is the observable in terms of 3, 4 or 5 particles, and:

- $M_{\mu\nu}g^{\mu\nu}$ is the cross section fo the production of the $q\bar{q}\gamma$ system plus a massive gluon with momentum k and mass λ
- $M_{\mu\nu}P^{\mu\nu}_{\text{split}}$ is the square amplitude for the production of $q\bar{q}\gamma$ plus a $q\bar{q}$ pair by a (massless virtual) gluon of momentum k ($k^2 = \lambda^2$) via splitting, but normalized so that

$$\int \mathrm{d}\Phi^{\mu\nu}_{\text{split}} P^{\mu\nu}_{\text{split}} = g^{\mu\nu} - k^\mu k^\nu/\lambda^2$$

- V_λ is the virtual corrections to the $\gamma^* \to q\bar{q}\gamma$ process, due to the exchange of a massive gluon.

Our new analytic findings can also be applied to shape variables.

The large-n_f, $T_O(\lambda)$ result can also be written as

$$T_O(\lambda) = N \int \mathrm{d}\Phi_3 \left\{ \int \mathrm{d}\Phi_k^{(\lambda)} M_{\mu\nu}(k) \left[\int \mathrm{d}\Phi_{\text{split}} \overbrace{P^{\mu\nu}_{\text{split}}(O_5 - O_4)}^{\Delta(\lambda)} + \overbrace{O_4 g^{\mu\nu}}^{R(\lambda)} \right] + \overbrace{V_\lambda O_3}^{V(\lambda)} \right\}.$$

We can rewrite it as

$$\begin{aligned} T_O(\lambda) \quad = \quad & N \int \mathrm{d}\Phi_3 \left\{ \int \mathrm{d}\Phi_k^{(\lambda)} M_{\mu\nu}(k) \left[\int \mathrm{d}\Phi_{\text{split}} P^{\mu\nu}_{\text{split}}(O_5 - O_4) + (O_4 - O_3) g^{\mu\nu} \right] \right. \\ & \left. + \left[\int \mathrm{d}\Phi_k^{(\lambda)} M_{\mu\nu} g^{\mu\nu} + V_\lambda \right] O_3 \right\}. \end{aligned}$$

Now, the second line contains the sum of the virtual plus an unrestricted integral in k of the massive real contribution.

By our findings, if the mapping $\Phi_3, \Phi_k^{(\lambda)}$ is smooth,

It does not have linear terms in λ!

Focus upon the first line:

$$T_O^{(\mathrm{first})}(\lambda) = N \int \mathrm{d}\Phi_3 \left\{ \int \mathrm{d}\Phi_k^{(\lambda)} M_{\mu\nu}(k) \left[\int \mathrm{d}\Phi_{\mathrm{split}} P_{\mathrm{split}}^{\mu\nu} (O_5 - O_4) + (O_4 - O_3) g^{\mu\nu} \right] \right\}$$

Since O is IR safe, there is one soft suppression from there. So, we can evaluate M neglecting $\mathcal{O}(1)$ terms in ω:

$$T_O^{(\mathrm{first})}(\lambda) \approx N \int \mathrm{d}\Phi_3 B \int \mathrm{d}\Phi_k^{(\lambda)} P_{\mu\nu}^{(\mathrm{soft})} \left[\int \mathrm{d}\Phi_{\mathrm{split}} P_{\mathrm{split}}^{\mu\nu} (O_5 - O_3) \right]$$

where we only need the Born cross section B, the soft emission tensor $P_{\mu\nu}^{(\mathrm{soft})}$, and the splitting factor $P_{\mathrm{split}}^{\mu\nu}$:

$$\begin{aligned} P_{\mu\nu}^{(\mathrm{soft})} &= \left(\frac{p_1^\mu}{(p_1+k)^2} - \frac{p_2^\mu}{(p_2+k)^2} \right) \left(\frac{p_1^\nu}{(p_1+k)^2} - \frac{p_2^\nu}{(p_2+k)^2} \right), \\ P_{\mathrm{split}}^{\mu\nu} &= N \, \mathrm{Tr}[\not{q} \gamma^\mu (\not{k} - \not{q}) \gamma^\nu] \,. \end{aligned}$$

We can evaluate numerically $T_O^{(\mathrm{first})}(\lambda) - T_O^{(\mathrm{first})}(0)$, (canceling the constant terms under the integral sign) to get the linear term.

The Milan Factor

Very early approaches [Dokshitzer,Webber,Marchesini 95] on non-perturbative corrections near the 2-jet limit suggested the formula

$$\mathrm{d}\eta\,\mathrm{d}^2 k_\perp \left(\frac{1}{k_\perp^2}\right) [O(P,k) - O(p)]\alpha(k_\perp)$$

where the first term is the invariant phase space for soft emission, the term in the round bracket is the amplitude for soft emission in the eikonal approximation in the radiating dipole rest frame, and the term in square bracket is the contribution of the observable.

The ambiguity associated with the integration near the Landau pole for α_s corresponds to the linear power correction.

For example:

$$
\begin{aligned}
1-T: \quad O(P,k)-O(p) &= \frac{k_\perp}{Q}\,\mathsf{exp}(-|\eta|), \quad \int \mathrm{d}\eta\ \mathsf{exp}(|\eta|) = 2, \\
C: \quad O(P,k)-O(p) &= \frac{k_\perp}{Q}\frac{3}{\mathsf{cosh}(\eta)}, \qquad \int \mathrm{d}\eta\, \frac{1}{\mathsf{cosh}(\eta)} = 3\pi
\end{aligned}
$$

These approaches ignored the gluon virtuality, that was set to zero in the formula, and the dependence of the shape variable upon the products of the gluon decaying into massless partons, that spoils the universality in the above formula [Seymour,PN,95].

Subsequently, Dokshitzer,Lucenti,Marchesini,Salam, 97-98 demonstrated that for a wide class of observables the inclusion of the gluon splitting process changed the original formula by a universal, constant factor, that was dubbed the Milan factor.

For this to hold, the observable must be additive under multiple soft emission, i.e.

$$O(P, k_1, \ldots, k_n) \approx O(P_1, k_1) + \ldots + O(P_n, k_n)$$

(among the early approaches, some advocated the use of a massive gluon [Akhoury,Zakarov,95]. This leads to different results, and their universality cannot be granted).

We found [Caola,Ferrario Ravasio,Limatola,Melnikov,Ozcelik,PN] that the also in the 3-jet limit the Milan factor formula can be derived (with the same Milan factor as in the 2-jet case)

$$|O|_{\rm NP} = \mathcal{M}\,\mathcal{I}_{\rm NP} \int {\rm d}\sigma_B(\Phi_B)\mathcal{T}^\lambda \left[\sum_{\rm dip} \int [{\rm d}k]\frac{M_S}{\alpha_S}\,\delta(|k_\perp|-\lambda)[O(\Phi_{B,k})-O(\Phi_B)]\right]$$

where $k^2=0$, and

$$[{\rm d}k]\frac{M_s}{\alpha_s} = \frac{{\rm d}^3k}{2k^0(2\pi^3)}C_{\rm dip}\frac{g_s^2}{\alpha_s}\frac{p_1\cdot p_2}{p_1\cdot k\, p_2\cdot k} = \frac{2C_{\rm dip}\alpha_S}{\pi}{\rm d}\eta\,\frac{{\rm d}\phi}{2\pi}\,\frac{{\rm d}k_\perp}{k_\perp}$$

- Notice the trade: $k^2=\lambda^2 \to k_\perp = \lambda$.
- The shape variable is evaluated for the extra-emission of one massless parton.
- The proof is not simple. However it is clear how the addittivity of the shape variable makes this possible.
- An extra condition emerges: the rapidity integral must converge.

For the cumulant of a shape variable, we obtain

$$\Sigma(v)_{\mathrm{NP}} = \left\{ \int \mathrm{d}\sigma_B(\Phi_B)\delta(v(\Phi_B) - v) \sum_{\mathrm{dip}} \left[-\mathcal{M} \frac{2C_{\mathrm{dip}}}{2\pi} \int \frac{\mathrm{d}\phi}{2\pi} \mathrm{d}\eta \, h_v(\eta, \phi) \right] \right\} \mathcal{I}_{\mathrm{NP}}$$

where

$$h_v(\eta, \phi) = \lim_{k_\perp \to 0} \left(\frac{Q}{|k_\perp|} \left[v(P, k) - v(p) \right] \right)$$

and the function h is easily calculable for the shape variables of interest.

From $\gamma^* \to q\bar{q}\gamma$ to $\gamma^* \to q\bar{q}g$

The calculation of the linear power corrections for the $\gamma^* \to q\bar{q}\gamma$ production process only involves the radiation from the $q\bar{q}$ dipole in the soft approximation.

This result suggests the generalization to the realistic $\gamma^* \to q\bar{q}g$, applying the soft approximation to this case.

Thus one can simply add the contributions arising from each one of the final state colour dipoles, i.e. $q\bar{q}$, qg and $\bar{q}g$.

Shape Variables of choice

Shape variables are IR stable functions of the final state kinematics. We consider:

- Thrust: $\tau = 1 - T$, $T = \max_{\hat{t}} \sum |\vec{p}_i \cdot \hat{t}| / \sum |\vec{p}_i|$
- C: $\Theta^{\alpha\beta} \sum_i \frac{p_i^\alpha p_i^\beta}{|\vec{p}_i|} / \sum_i |\vec{p}_i|$, $C = 3(\lambda_1\lambda_2 + \lambda_1\lambda_3 + \lambda_2\lambda_3)$
- y_3: take Durham jet clustering, with distance measure $y_{ij} = 2min(E_i^2, E_j^2)(1 - \cos\theta_{ij})/Q^2$. Then y_3 is define as the value of y_{ij} at the clustering step that leads to the transition from 3 to 2 clusters.
- Mh2 (heavy jet mass): the heaviest of the squared masses of the two hemisperes defined by the plane orthogonal to the thrust axis, normalized to Q^2
- Md2: the heaviest minus the lightes of the squared masses of the two hemisperes, normalized to Q^2.
- Bw: $\max(B_1, B_2)$, $B_i = \sum_{p_k \in H_i} |\vec{p}_k \times \hat{t}| / (2 \sum_i |\vec{p}_i|)$.

Non-perturbative corrections can be parametrized as a shift in the perturbative cumulant distribution:

$$\Sigma(s) \longrightarrow \Sigma(s + H_{\mathrm{NP}}\zeta(s)), \quad \text{where} \quad \Sigma(s) = \int \mathrm{d}\sigma(\Phi)\theta(s - s(\Phi))$$

and $H_{\mathrm{NP}} \approx \Lambda/Q$ is a non-perturbative parameter that must be fitted to data.

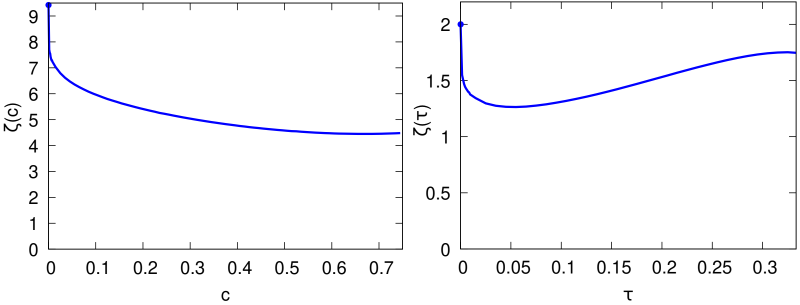

The dot in the plots represents the constant value that was used in earlier studies. The value of $\zeta(c)$ at the symmetric point $c = 3/4$ was also computed by Luisoni,Monni,Salam 2021.

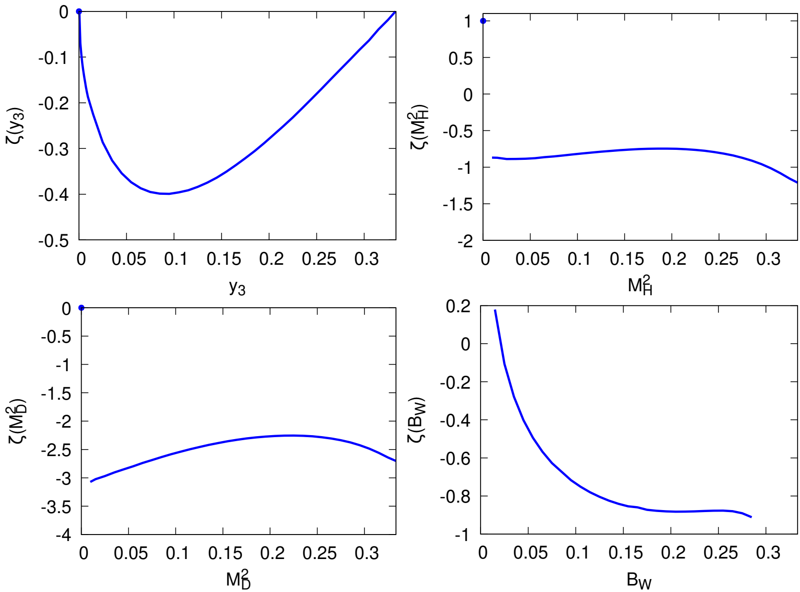

(G.Zanderighi,PN2023) In some cases ζ is negative!

Rapid variations near $v = 0$

Near $v = 0$, the Born amplitude is dominated by the soft-collinear region.

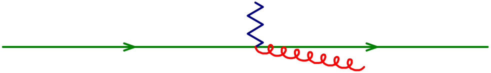

$$\text{radiation} = \frac{C_A}{2} M_{\bar{q}g} + \frac{C_A}{2} M_{qg} + \left(C_F - \frac{C_A}{2} \right) M_{q\bar{q}}$$

but $M_{qg} \approx 0$, $M_{\bar{q}g} \approx M_{q\bar{q}}$, so the total is $\approx C_F M_{q\bar{q}}$.

Our $\zeta(v)$ functions, for $v \to 0$ MUST approach the 2-jet limit value; but up to single logs!, i.e. terms of relative order $1/|\log(v)|$.

Singularity at the origin

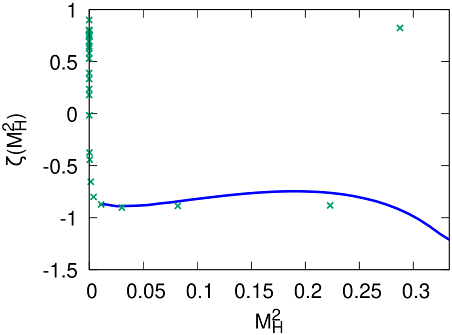

Insist on $v \to 0$ (quadruple precision, log scale histogram). Two-jet limit reached, but subleading terms are extremely important! Singularity compatible with a form

$$\frac{\frac{\log v + C}{v}}{\frac{\log v + B}{v}}$$

for $B \neq C$.

α_s from e^+e^- shape variables

- Historically the framework of choice to measure α_s directly from the $q\bar{q}g$ vertex.
- In practice: very convincing at the 10% level; affected by non-perturbative uncertainties if one wants higher precision
- $\alpha_s(M_Z)$ from NNLO+NLL+Monte Carlo models:
  - 0.1224 ± 0.0039 ALEPH 2009, [arXiv:0906.3436].)
  - 0.1189 ± 0.0043 OPAL 2011, [arXiv:1101.1470])
  - 0.1172 ± 0.0051 JADE 2009, [arXiv:0810.1389]

The use of Monte Carlo models to correct for hadronization effects have long been criticized, since the interplay of perturbative and non-perturbative effects in Shower Monte Carlo is not fully clear.

α_s from e^+e^- shape variables

As an alternative, another class of determinations is based upon analytic modeling of non-perturbative effects, using methods like SCET, dispersive models and low scale QCD effective couplings, and using NNLO+N^{3}LL calculations:

- 0.1135 ± 0.0011 R.Abbate *et al*, 2011, [arXiv:0809.3326]
- $0.1134 \begin{array}{l} +0.0031 \\ -0.0025 \end{array}$ Gehrmann,Luisoni,Monni, 2013,[arXiv:1210.6945]
- 0.1123 ± 0.0015 Hoang *et al*, 2015 [arXiv:1501.04111]

They tend to result in a rather low value, not in good agreement with world data.

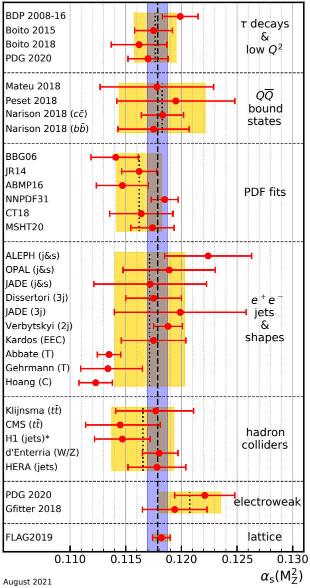

Results from Zanderighi, PN 2023

Simultaneous fit to C, t and y_3, both for our newly computed $\zeta(v)$, and, for comparison, with $\zeta(v) \to \zeta_{2J}(v) = \zeta(0)$ (traditional method for the computation of power corrections).

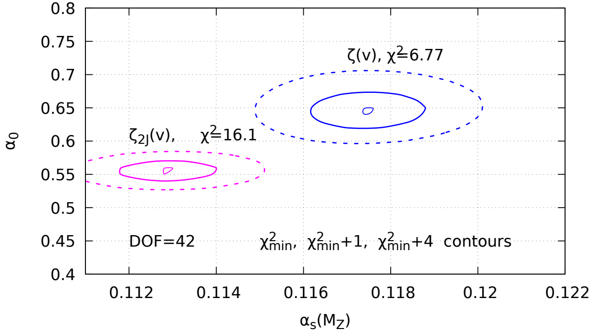

The central value is at $\alpha_s(M_Z) = 0.1174$, $\alpha_0 = 0.64$. The "traditional" method leads to smaller values of α_s.

Results from Zanderighi, PN 2023

Individual fits:

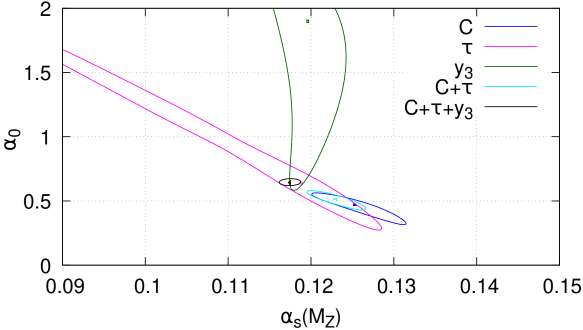

Only the combination of the three observables leads to a sensible determination of α_s

Extension of 2023 result (with G. Zanderighi)

Inclusion of all data we could find at all energies

DELPHI 91.2 45 66 76 133 161 172 183 189 192 196 200 202 205 207
ALEPH 91.2 133 161 172 183 189 200 206
OPAL 91.2 133 177 197
L3 91.2 41.4 55.3 65.4 75.7 82.3 85.1 130.1
136.1 161.3 172.3 182.8 188.6 194.4 200
JADE 22 35 44
TRISTAN 58
JADEOPAL 91.2 35 44 133 161 172 183 189
SLD 91.2

- We perform the fits at the central scale, and then consider its variations by a factor of 2 below and above.
- In order to get a better fit of the very precise Z-peak data, we chose the central scale to be a function of the shape variable:
  We first compute the average k_T as a function of the value of each shape variable (computed at the LO level), and then choose the k_T as central value of the scale. Fitting only ALEPH data on the Z peak we get:

	χ^2/dof	best μ_R	$\alpha_S(M_Z)$	α_0
fixed scale	2.5	$0.175 \times M_Z$	0.1170	0.58
running scale	1.66	$1.28 \times \langle k_T \rangle$	0.1168	0.593

  (best μ_R leads to the lowest χ^2)
- The lower limit in the fit range is taken at twice the Sudakov peak position. Upper limit is 0.6 for C and 0.3 for thrust and y3.

Fitting Thrust, C-parameter and y_3 at the same time

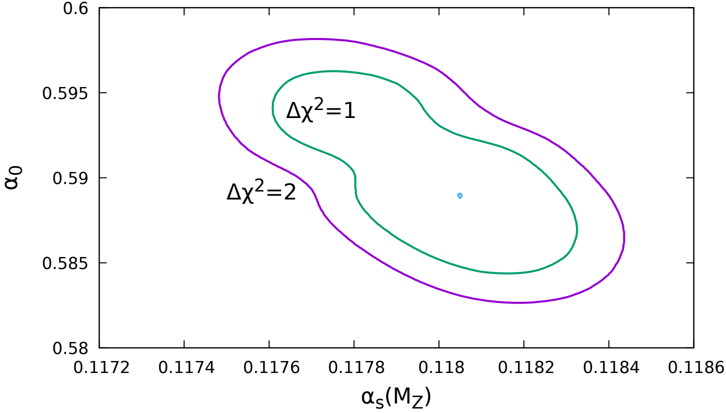

Leading to $\alpha_s(M_Z) = 0.1180$, and $\alpha_0 = 0.589$, with $\chi^2 = 1125.7$ over 895 degrees of freedom ($\chi^2/\mathrm{dof} = 1.258$).

Fits to individual observables: C

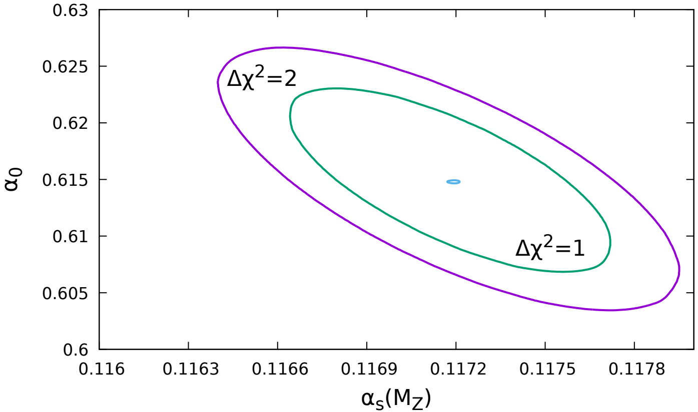

$\alpha_s(M_Z) = 0.1172$, and $\alpha_0 = 0.6148$, with $\chi^2 = 269.0$ over 292 degrees of freedom ($\chi^2/\mathrm{dof} = 0.921$).

Fits to individual observables: T

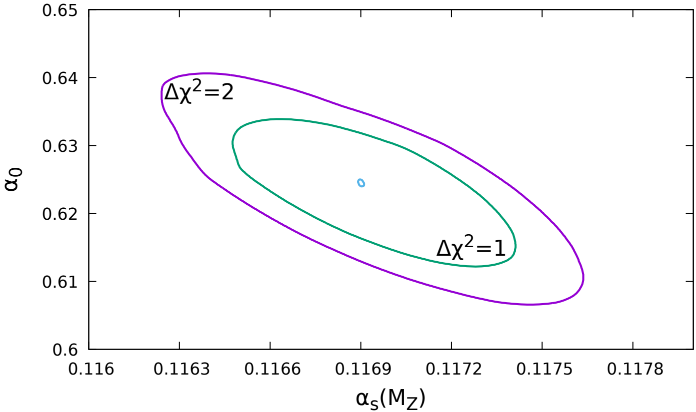

$\alpha_s(M_Z) = 0.1169$, and $\alpha_0 = 0.6245$, with $\chi^2 = 651.7$ over 151 degrees of freedom ($\chi^2/\mathrm{dof} = 1.442$).

Fits to individual observables: $y3$

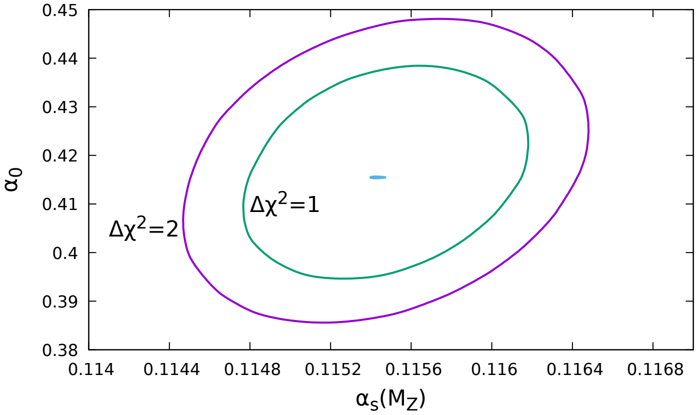

$\alpha_s(M_Z) = 0.1155$, and $\alpha_0 = 0.4151$, with $\chi^2 = 71.6$ over 292 degrees of freedom ($\chi^2/\mathrm{dof} = 0.474$).

All together

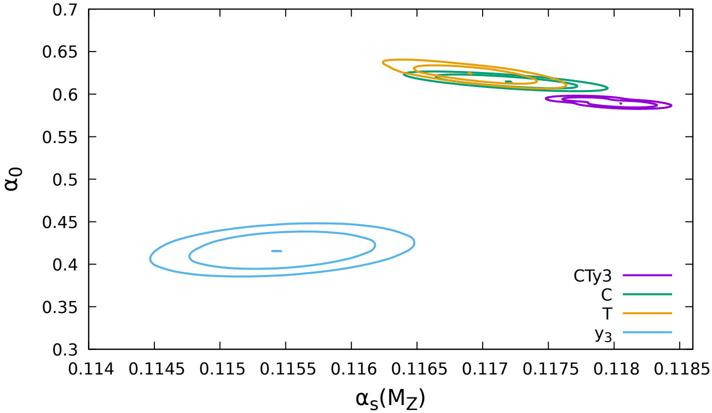

		Global Fit		Individual Fits	
Obs.	Dof	χ^2	χ^2/dof	χ^2	χ^2/dof
C	292	278.2	0.95	269.0	0.921
T	452	659.7	1.465	651.7	1.44
y_3	151	132.7	0.879	71.6	0.47

- For C and T, individual fits are compatible with the CTy3 fit,
- For y_3 a much smaller α_0 is favoured.
- The χ^2 for the individual y_3 fit is very low, so that a larger value of α_0 (leading to a larger value of α_s) is also acceptable.
- The inclusion of y_3 in the CTy3 fit pulls α_0 to smaller values, and thus increases α_s slightly.

Variations: global fit CTy3

Variation	$\alpha_s(M_Z)$	α_0	χ^2	χ^2/dof	dof
Central	0.1180	0.5892	1125.6976	1.2578	895
High scale	0.1167	0.5846	1465.9393	1.6021	915
Low scale	0.1167	0.6683	1940.0007	2.3775	816
Std scheme	0.1173	0.5347	1090.8732	1.2202	894
p scheme	0.1160	0.5624	1051.1005	1.1757	894
D scheme	0.1199	0.7252	747.3571	0.8350	895
high low-lim	0.1177	0.5673	947.3134	1.2498	758
low low-lim	0.1165	0.6260	1579.9496	1.6073	983
non-pert scheme 2	0.1193	0.5923	1249.1436	1.3957	895
non-pert scheme 3	0.1189	0.5825	1232.5919	1.3772	895
non-pert scheme 4	0.1185	0.5927	1158.0191	1.2939	895
minus non-pert error	0.1187	0.5865	1122.1407	1.2538	895
plus non-pert error	0.1189	0.5649	1228.4413	1.3726	895

We have considered:

- Scale variations, up and down by a factor of 2 from default
- Mass scheme: how to solve the ambiguity in shape variables due to hadron masses [Salam,Wicke,2001]. We use as default the E scheme; variations: std. scheme, p scheme and D scheme.
- Range low limit: 2 (default), 1.7, 3 times the peak position.
- 4 different ways to implement NP corrections: shift in the full cumulant with or without adding an estimate of quadratic terms; shift in the LO cumulant; expand the correction around the perturbattive value. cumulant argument
- Subtract NP error
- Add NP error

In all cases we find the mass scheme issue very disturbing (slightly less than a 2% correction in both directions.

2-jet NP correction, fit CTy3

Variation	$\alpha_s(M_Z)$	α_0	χ^2	χ^2/dof	dof
Central	0.1161	0.5389	1149.9394	1.2848	895
High scale	0.1150	0.5181	1830.6507	2.0007	915
Low scale	0.1155	0.6061	1523.6604	1.8672	816
Std scheme	0.1153	0.4989	1106.6396	1.2379	894
p scheme	0.1141	0.5119	1125.7113	1.2592	894
D scheme	0.1173	0.6465	923.2022	1.0315	895
high low-lim	0.1159	0.5325	977.2551	1.2893	758
low low-lim	0.1143	0.5658	1510.5800	1.5367	983
non-pert scheme 2	0.1163	0.5603	1281.1125	1.4314	895
non-pert scheme 3	0.1167	0.5305	1312.8618	1.4669	895
non-pert scheme 4	0.1161	0.5390	1149.9904	1.2849	895
minus non-pert error	0.1161	0.5390	1150.0007	1.2849	895
plus non-pert error	0.1161	0.5389	1149.8783	1.2848	895

Everything else being equal, we found that using the two-jet limit NP correction lowers the value of α_s by nearly 0.002 in the CTy3 fit.

For all fits:

	$\alpha_s(M_Z)$							
	CTy3		C		T		y_3	
Variation	$\zeta(v)$	$\zeta(0)$	$\zeta(v)$	$\zeta(0)$	$\zeta(v)$	$\zeta(0)$	$\zeta(v)$	$\zeta(0)$
Central	.1181	.1161	.1169	.1139	.1168	.1158	.1155	.1154
High scale	.1167	.1150	.1212	.1184	.1208	.1191	.1157	.1161
Low scale	.1167	.1155	.1141	.1105	.1159	.1128	.1122	.1131
Std scheme	.1173	.1153	.1164	.1118	.1152	.1148	.1150	.1149
p scheme	.1160	.1141	.1164	.1118	.1152	.1148	.1137	.1135
D scheme	.1199	.1173	.1190	.1153	.1205	.1170	.1156	.1166
high low-lim	.1177	.1159	.1221	.1116	.1180	.1172	.1142	.1154
low low-lim	.1165	.1143	.1151	.1116	.1154	.1133	.1154	.1142

Stronger decrease for C, less for T, almost none for y_3.

M_h^2 and M_d^2

- These observables have $\zeta(v) < 0$ in most of the range, with an effective large jump near the origin. They are not easy to fit as the others, perhaps because of this jump.
- Unfortunately, the data is inconsistent for these observables, with DELPHI differing strongly from all other experiments.
- An independent analysis of DELPHI data on the Z peak [Daniel Wicke, 1999 (thesis)] is instead consistent with the other experiments.

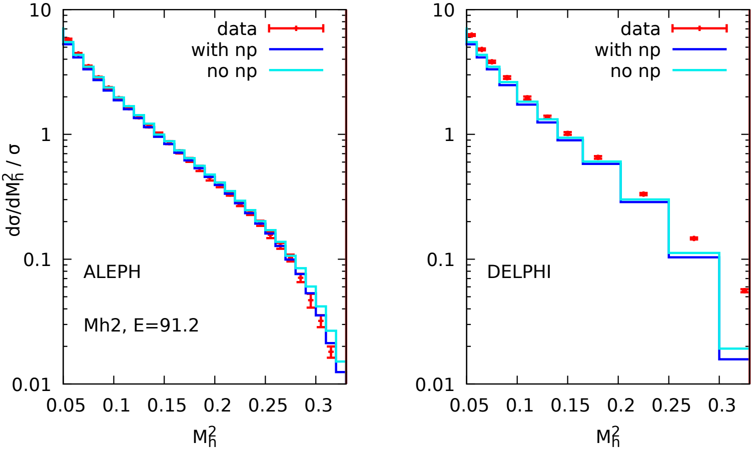

10
1
0.1
0.01
data
with np
no np
ALEPH
Mh2, E=91.2
$d\sigma/dM_h^2$ / σ
0.05
0.1
0.15
0.2
0.25
0.3
M_h^2
10
1
0.1
0.01
data
with np
no np
DELPHI
0.05
0.1
0.15
0.2
0.25
0.3
M_h^2

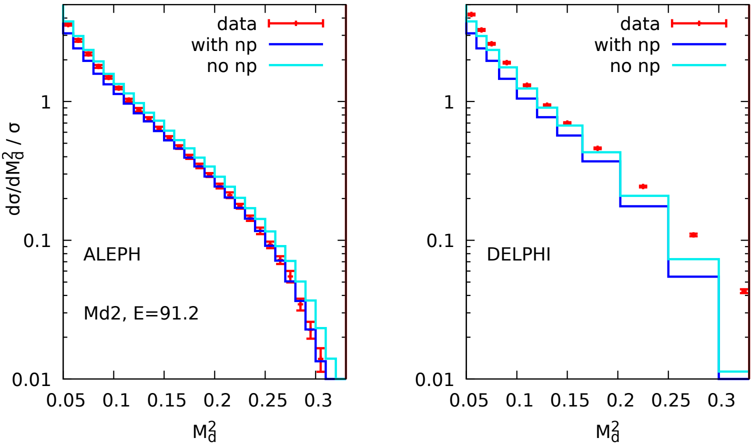
data
with np
no np
ALEPH
Md2, E=91.2
DELPHI
$d\sigma/dM_d^2 / \sigma$
M_d^2
1
0.1
0.01
0.05
0.1
0.15
0.2
0.25
0.3

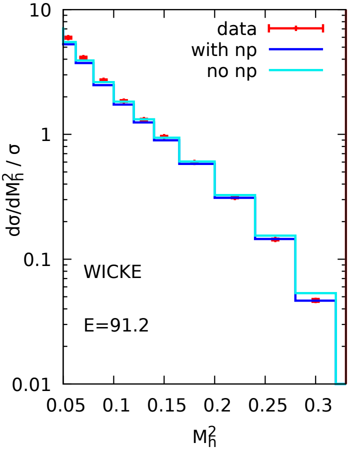
10
1
0.1
0.01
dσ/dM$_h^2$ / σ
data
with np
no np
WICKE
E=91.2
0.05
0.1
0.15
0.2
0.25
0.3
M$_h^2$

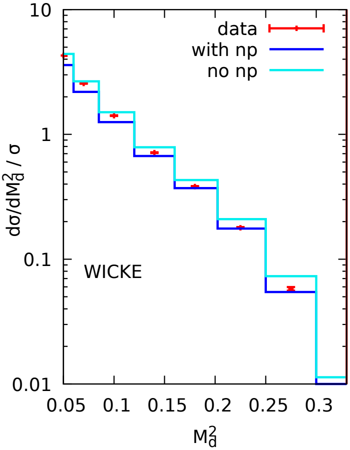
10
1
0.1
0.01
dσ/dM$_d^2$ / σ
data
with np
no np
WICKE
0.05
0.1
0.15
0.2
0.25
0.3
M$_d^2$

Including M_h^2 and M_d^2 in the fit

Variation	$\alpha_s(M_Z)$	α_0	χ^2	χ^2/dof	dof
Central	0.1222	0.5273	2326.9662	2.6716	871
High scale	0.1217	0.5518	3792.5798	4.3543	871
Low scale	0.1203	0.5200	5082.6673	6.2135	818
Std scheme	0.1207	0.4435	5898.7965	6.8115	866
p scheme	0.1197	0.5076	2108.0830	2.4231	870
D scheme	0.1260	0.6058	2913.3330	3.3448	871
high low-lim 3	0.1210	0.5342	1717.8313	2.3120	743
high low-lim 4	0.1204	0.5519	1387.2944	2.2091	628
high low-lim 5	0.1201	0.5663	1109.9750	2.0864	532
low low-lim	0.1229	0.5302	3817.7635	3.9977	955
non-pert scheme 2	0.1244	0.5030	4255.4882	4.8857	871
non-pert scheme 3	0.1241	0.5101	3939.7764	4.5233	871
non-pert scheme 4	0.1225	0.5246	2428.3917	2.7881	871
minus non-pert error	0.1224	0.5246	2361.0027	2.7107	871
plus non-pert error	0.1220	0.5302	2295.3221	2.6353	871

Including M_h^2 and M_d^2 in the fit, 2-jets NP corrections

Variation	$\alpha_s(M_Z)$	α_0	χ^2	χ^2/dof	dof
Central	0.1171	0.6194	7003.1054	8.0403	871
High scale	0.1072	0.6829	14792.3877	16.9832	871
Low scale	0.1150	0.6638	2923.2290	3.5736	818
Std scheme	0.1162	0.5106	6005.4771	6.9347	866
p scheme	0.1121	0.6216	7133.7624	8.1997	870
D scheme	0.1191	0.7231	11292.6068	12.9651	871
high low-lim	0.1142	0.6993	5577.2908	7.5064	743
low low-lim	0.1168	0.6176	7483.8707	7.8365	955
non-pert scheme 2	0.1268	0.5277	9499.9953	10.9070	871
non-pert scheme 3	0.1264	0.5263	9457.7652	10.8585	871
non-pert scheme 4	0.1171	0.6195	7004.0344	8.0414	871
minus non-pert error	0.1171	0.6195	7004.1066	8.0415	871
plus non-pert error	0.1171	0.6194	7002.1081	8.0392	871

CONCLUSIONS

- Something new has been understood in the framework of power corrections for collider processes.
- Applications in e^+e^- shape variables seem to support these findings to some extent.
- Prospects for fits to α_s in e^+e^- framework are unclear because of:
  - Hadron mass effects are poorly understood.
  - Interplay of (new) NP corrections and resummation needs more work
  - Possible inconsistencies between experiments should be carefully assessed.
  - Correlations in data (and theory) needs a better treatment.

BACKUP

Variations: fit CT

Variation	$\alpha_s(M_Z)$	α_0	χ^2	χ^2/dof	dof
Central	0.1175	0.6061	953.0331	1.2810	744
High scale	0.1211	0.5013	998.3168	1.3418	744
Low scale	0.1146	0.7534	969.7802	1.3756	705
Std scheme	0.1157	0.5710	908.7845	1.2231	743
p scheme	0.1157	0.5710	908.7845	1.2231	743
D scheme	0.1198	0.7300	609.9992	0.8199	744
high low-lim	0.1190	0.5421	809.1090	1.3286	609
low low-lim	0.1157	0.6444	1166.3332	1.4224	820
non-pert scheme 2	0.1191	0.6126	966.5737	1.2992	744
non-pert scheme 3	0.1192	0.5852	971.5030	1.3058	744
non-pert scheme 4	0.1171	0.6341	950.4401	1.2775	744
minus non-pert error	0.1170	0.6271	943.4099	1.2680	744
plus non-pert error	0.1175	0.5947	969.2549	1.3028	744

Variations: fit C

Variation	$\alpha_s(M_Z)$	α_0	χ^2	χ^2/dof	dof
Central	0.1172	0.6148	268.9646	0.9211	292
High scale	0.1212	0.5076	276.6518	0.9474	292
Low scale	0.1141	0.7634	281.2422	0.9868	285
Std scheme	0.1164	0.5639	336.3641	1.1519	292
p scheme	0.1164	0.5639	336.3641	1.1519	292
D scheme	0.1190	0.7340	192.4281	0.6590	292
high low-lim	0.1221	0.4447	193.9756	0.8857	219
low low-lim	0.1151	0.6469	349.1941	1.0362	337
non-pert scheme 2	0.1191	0.6189	274.3330	0.9395	292
non-pert scheme 3	0.1195	0.5902	274.5646	0.9403	292
non-pert scheme 4	0.1170	0.6406	270.9737	0.9280	292
minus non-pert error	0.1173	0.6306	264.9847	0.9075	292
plus non-pert error	0.1172	0.6039	273.1821	0.9356	292

Variations: fit T

Variation	$\alpha_s(M_Z)$	α_0	χ^2	χ^2/dof	dof
Central	0.1169	0.6245	651.7492	1.4419	452
High scale	0.1208	0.5253	687.2753	1.5205	452
Low scale	0.1159	0.7082	639.8972	1.5236	420
Std scheme	0.1152	0.5876	534.0098	1.1841	451
p scheme	0.1152	0.5876	534.0098	1.1841	451
D scheme	0.1205	0.7232	372.8273	0.8248	452
high low-lim	0.1180	0.5896	596.8003	1.5303	390
low low-lim	0.1154	0.6672	713.4200	1.4771	483
non-pert scheme 2	0.1185	0.6557	660.7301	1.4618	452
non-pert scheme 3	0.1192	0.5888	672.7682	1.4884	452
non-pert scheme 4	0.1160	0.6758	647.1783	1.4318	452
minus non-pert error	0.1165	0.6506	648.7400	1.4353	452
plus non-pert error	0.1172	0.6038	662.0738	1.4648	452

Variations: fit y3

Variation	$\alpha_s(M_Z)$	α_0	χ^2	χ^2/dof	dof
Central	0.1155	0.4151	71.6269	0.4744	151
High scale	0.1157	0.5223	274.9637	1.6080	171
Low scale	0.1122	0.0324	58.7413	0.5292	111
Std scheme	0.1150	0.4011	77.0834	0.5105	151
p scheme	0.1137	0.4032	66.6759	0.4416	151
D scheme	0.1168	0.4999	58.3885	0.3867	151
high low-lim	0.1156	0.4192	69.9605	0.4695	149
low low-lim	0.1142	0.3729	95.8462	0.5880	163
non-pert scheme 2	0.1154	0.4152	75.5347	0.5002	151
non-pert scheme 3	0.1154	0.4163	74.9921	0.4966	151
non-pert scheme 4	0.1155	0.4144	71.7165	0.4749	151
minus non-pert error	0.1157	0.4323	70.6969	0.4682	151
plus non-pert error	0.1153	0.3588	69.4217	0.4597	151

2-jet NP correction, fit CT

Variation	$\alpha_s(M_Z)$	α_0	χ^2	χ^2/dof	dof
Central	0.1173	0.5279	1015.4571	1.3649	744
High scale	0.1209	0.4524	1061.9594	1.4274	744
Low scale	0.1138	0.6443	1036.7306	1.4705	705
Std scheme	0.1157	0.4976	980.6222	1.3198	743
p scheme	0.1157	0.4976	980.6222	1.3198	743
D scheme	0.1194	0.6249	716.3991	0.9629	744
high low-lim	0.1202	0.4563	838.0689	1.3761	609
low low-lim	0.1142	0.5689	1361.1738	1.6600	820
non-pert scheme 2	0.1189	0.5234	1029.5211	1.3838	744
non-pert scheme 3	0.1190	0.5085	1032.0306	1.3871	744
non-pert scheme 4	0.1173	0.5279	1015.4754	1.3649	744
minus non-pert error	0.1173	0.5279	1015.4595	1.3649	744
plus non-pert error	0.1173	0.5279	1015.4547	1.3649	744

2-jet NP correction, fit C

Variation	$\alpha_s(M_Z)$	α_0	χ^2	χ^2/dof	dof
Central	0.1139	0.5696	252.2759	0.8640	292
High scale	0.1184	0.4866	262.1126	0.8976	292
Low scale	0.1105	0.6708	259.6847	0.9112	285
Std scheme	0.1118	0.5428	324.8358	1.1125	292
p scheme	0.1118	0.5428	324.8358	1.1125	292
D scheme	0.1153	0.6616	176.5806	0.6047	292
high low-lim	0.1116	0.6221	185.3429	0.8463	219
low low-lim	0.1116	0.5890	325.2677	0.9652	337
non-pert scheme 2	0.1176	0.5458	271.2322	0.9289	292
non-pert scheme 3	0.1172	0.5305	272.4936	0.9332	292
non-pert scheme 4	0.1139	0.5696	252.2884	0.8640	292
minus non-pert error	0.1139	0.5696	252.2500	0.8639	292
plus non-pert error	0.1139	0.5696	252.3017	0.8640	292

2-jet NP correction, fit T

Variation	$\alpha_s(M_Z)$	α_0	χ^2	χ^2/dof	dof
Central	0.1158	0.5616	669.2086	1.4805	452
High scale	0.1191	0.4946	709.5784	1.5699	452
Low scale	0.1128	0.6683	613.5789	1.4609	420
Std scheme	0.1148	0.5210	561.5604	1.2451	451
p scheme	0.1148	0.5210	561.5604	1.2451	451
D scheme	0.1170	0.6799	380.7676	0.8424	452
high low-lim	0.1172	0.5355	607.7026	1.5582	390
low low-lim	0.1133	0.6078	737.7402	1.5274	483
non-pert scheme 2	0.1184	0.5559	682.2518	1.5094	452
non-pert scheme 3	0.1191	0.5190	694.5941	1.5367	452
non-pert scheme 4	0.1158	0.5616	669.2343	1.4806	452
minus non-pert error	0.1158	0.5616	669.2362	1.4806	452
plus non-pert error	0.1158	0.5616	669.1810	1.4805	452

2-jet NP correction, fit y3

Variation	$\alpha_s(M_Z)$	α_0	χ^2	χ^2/dof	dof
Central	0.1154		67.9599	0.4501	151
High scale	0.1161		330.6187	1.9334	171
Low scale	0.1131		104.3764	0.9403	111
Std scheme	0.1149		72.9595	0.4832	151
p scheme	0.1135		63.5661	0.4210	151
D scheme	0.1166		61.0976	0.4046	151
high low-lim	0.1154		66.6631	0.4474	149
low low-lim	0.1142		88.6679	0.5440	163
non-pert scheme 2	0.1154		67.9599	0.4501	151
non-pert scheme 3	0.1154		67.9599	0.4501	151
non-pert scheme 4	0.1154		67.9599	0.4501	151
minus non-pert error	0.1154		67.9599	0.4501	151
plus non-pert error	0.1154		67.9599	0.4501	151

Processes with massive partons

The generic statement that can be made for massless partons cannot be generalized to the massive case. Nevertheless, with a reasoning inspired by the Low-Burnett-Kroll theorem, some results can be obtained also in this case. In particular:

- The absence of linear renormalons can be derived for B meson decays, as long as the B mass is expressed in a short-distance scheme (like the $\overline{\mathrm{MS}}$ one). This result was already obtained by Beneke, and it also follows from the existance of an OPE for includive B decays.
- The absence of linear renormalon in the t-channel, total single top cross section (if m_t is in a short distance scheme!), and the computation of linear corrections in the top differential distributions.
- The absence of linear renormalons in $q\bar{q} \to t\bar{t}$ total cross section (again with m_t in a short distance scheme), and the computation of linear corrections in the top differential distributions.

Single Top

The result for the differential distribution can be expressed as a shifts in the argument of the Born cross section. For the transverse momentum and rapidity of the top the shift are given by

$$\begin{aligned}\frac{\delta_{\mathrm{NP}}[p_\perp]}{p_\perp} &= \frac{\alpha_s C_F}{2\pi}\frac{\pi\lambda}{m_t} \\ \delta_{\mathrm{NP}}[y_t] &= \frac{\alpha_s C_F}{2\pi}\frac{\pi\lambda}{m_t} \times \frac{8m_t^2\, s\, ch^2(y_t)}{(s+m_t^2)^2}\end{aligned}$$

Since we have

$$\frac{\delta_{\mathrm{NP}} m_t}{m_t} = \frac{\alpha_s C_F}{2\pi}\frac{\pi\lambda}{m_t}$$

we can use current determination of the top quark pole mass renormalon uncertainty $\delta_{\mathrm{NP}} m_t = 0.1 - 0.2$ GeV to estimate these effects.

$q\bar{q} \to t\bar{t}$

The results have a more interesting structure

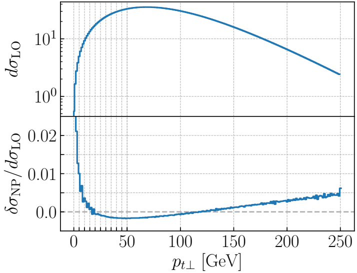

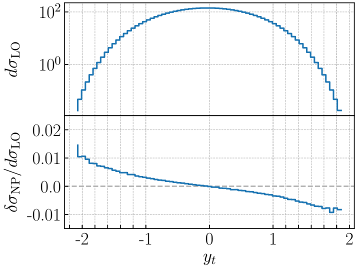

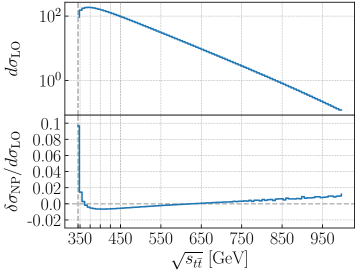

For example, for the p_t distribution

$$\frac{\delta_{\mathrm{NP}}[p_\perp]}{p_\perp} = \frac{\alpha_s C_F}{2\pi} \frac{\pi\lambda}{m_t} \frac{2C_F s_{t\bar{t}} - C_A 4m_t^2}{2(s_{t\bar{t}} - 4m_t^2)},$$

with an enhancement near threshold and a change of sign depending upon a colour factor combination.